References

[1] B. D. H. Tellegen, "The gyrator, a new electric network element," *Philips Res. Repts.*, vol. 3, pp. 81–101, April 1948.
[2] C. L. Hogan, "The microwave gyrator," *Bell Sys. Tech. J.*, vol. 31, p. 1, January 1952.
[3] N. G. Sakiotis and H. N. Chait, "Properties of ferrites in waveguides," *IRE Trans. Microwave Theory and Techniques*, vol. MTT-1, pp. 11–16, November 1953.
[4] H. N. Chait and T. R. Curry, "Y-circulator," *J. Appl. Phys. (Suppl.)*, vol. 30, pp. 152S–153S, March 1959.
[5] W. H. von Aulock, "Selection of ferrite materials for microwave device applications," *IEEE Trans. Magnetics*, vol. MAG-2, pp. 251–255, September 1966.
[6] H. Bosma, "On stripline Y-circulation at UHF," *IEEE Trans. Microwave Theory and Techniques*, vol. MTT-12, pp. 61–72, January 1964.
[7] J. B. Davies, "An analysis of the m-port symmetrical H-plane waveguide junction with central ferrite post," *IRE Trans. Microwave Theory and Techniques*, vol. MTT-10, pp. 596–604, November 1962.
[8] H. J. Butterweck, "Der Y-Zirkulator," *Arch. Elekt. Übertragung*, vol. 17, pp. 163–176, April 1963.
[9] E. Schwartz, "Broadband matching of resonant circuits and circulators," *IEEE Trans. Microwave Theory and Techniques*, vol. MTT-16, pp. 158–165, March 1968.
[10] C. E. Fay and R. L. Comstock, "Operation of the ferrite junction circulator," *IEEE Trans. Microwave Theory and Techniques*, vol. MTT-13, pp. 15–27, January 1965.
[11] L. K. Anderson, "An analysis of broadband circulators with external tuning elements," *IEEE Trans. Microwave Theory and Techniques*, vol. MTT-15, pp. 42–47, January 1967.
[12] G. L. Matthaei, L. Young, and E. M. T. Jones, *Microwave Filters, Impedance Matching Networks, and Coupling Structures*. New York: McGraw-Hill, 1964.
[13] Y. Konishi, "Lumped element Y circulator," *IEEE Trans. Microwave Theory and Techniques*, vol. MTT-13, pp. 852–864, November 1965.
[14] H. Bosma, "Performance of lossy H-plane Y circulators," *IEEE Trans. Magnetics*, vol. MAG-2, pp. 273–277, September 1966.
[15] V. E. Dunn and R. W. Roberts, "New design techniques for miniature VHF circulators," *Digest G-MTT Internat'l Microwave Symp.* (Clearwater, Fla., 1965), pp. 147–151.
[16] H. Bosma, "Theoretical aspects of 3-port junction circulators," *Digest G-MTT Internat'l Microwave Symp.* (Palo Alto, Calif., 1966), pp. 261–263.
[17] B. Lax and K. J. Button, *Microwave Ferrites and Ferrimagnetics*. New York: McGraw-Hill, 1962.
[18] Q. H. F. Vrehen, "Absorption and dispersion in porous and anisotropic polycrystalline ferrites at microwave frequencies" (*Digest*), this issue, p. 479.
[19] L. v.d. Kint, Philips Elcoma Ceramic Laboratories, Eindhoven, The Netherlands, private communication.
[20] G. P. Rodrigue, J. L. Allen, L. J. Lavedan, and D. R. Taft, "Operating dynamics and performance limitations of ferrite digital phase shifters," *IEEE Trans. Microwave Theory and Techniques*, vol. MTT-15, pp. 709–713, December 1967.
[21] F. Betts, D. H. Temme, and J. A. Weiss, "A switching circulator: S-band; stripline, remanent; 15 kilowatts; 10 microseconds; temperature-stable," *IEEE Trans. Microwave Theory and Techniques*, vol. MTT-14, pp. 665–669, December 1966.
[22] P. C. Goodman, "A latching ferrite junction circulator for phased array switching applications," *Digest G-MTT Internat'l Microwave Symp.* (Clearwater, Fla., 1965), pp. 123–126.
[23] J. B. Thaxter and G. S. Heller, "Circulators at 70 and 140 kMc," *Proc. IRE (Correspondence)*, vol. 48, pp. 110–111, January 1960.
[24] J. L. Allen, "Transient behavior of ferrite devices" (*Digest*), this issue, p. 607.

Magnetostatic Modes in Axially Magnetized Polycrystalline YIG Rods at 9.96 GHz

CARL E. PATTON AND ERNST SCHLÖMANN

Abstract—A large number of magnetostatic mode resonances have been observed in axially magnetized cylindrical rods at 9.96 GHz. The data can be satisfactorily explained on the basis of magnetostatic mode theory of volume and surface modes for rods in air and surface modes for rods encased in metal sleeves. The resonances were observed by inserting 0.075-inch diameter polycrystalline YIG rods through holes in a shorted TE_{10} rectangular waveguide section one half wavelength from the short so that the portion of the rod inside the waveguide was in a region of uniform microwave field, and measuring reflected microwave power as a function of static magnetic field strength with the field applied parallel to the rod axis. With the rod supported by 1-inch long metal sleeves on both sides of the waveguide, the spectrum consists of a series of weak resonances from 1800 to 2600 Oe, a main peak at 2725 Oe, and a series of resonances, decreasing in intensity with increasing field, above the main peak. By removing the sleeves and supporting the rod with dielectric inserts in the waveguide wall, the weak resonances were eliminated from the spectra. The positions of the observed peaks were found to agree with predictions from magnetostatic mode theory. The resonances on the low field side of the main peak correspond to surface modes excited in the sleeve-enclosed portions of the rod with an integral number of half wavelengths along the sleeve length. The main resonance corresponds to the excitation of a surface mode excited in the portion of the rod which is in the waveguide. The resonances on the high field side of the main peak correspond to volume modes excited in the portion of the rod which is in the waveguide.

Manuscript received March 1, 1968; revised May 2, 1968. Paper 17.9, presented at the 1968 INTERMAG Conference, Washington, D. C., April 3–5.

The authors are with the Research Division, Raytheon Company, Waltham, Mass.

I. Introduction

THERE HAS been considerable interest in magnetostatic mode phenomena for ferromagnetic insulators of rod geometry, primarily because of the potential applicability of these phenomena to magnetic delay lines at microwave frequencies. Consequently, much of the experimental work which has been reported has been device oriented [1], [2]. Only a few investigations [3], [4] have been concerned with the experimental observation of

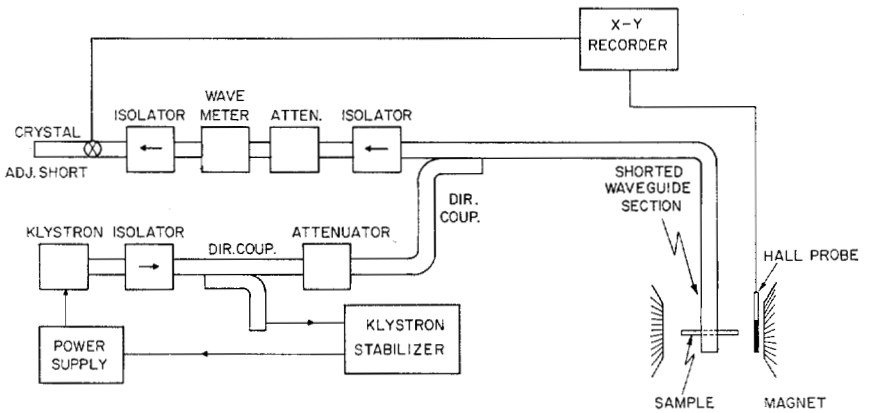

Fig. 1. Microwave instrumentation for the observation of magnetostatic mode resonances in axially magnetized rods at 9.96 GHz.

magnetostatic mode resonances in rods and the interpretation of the observed spectra in terms of previous theoretical developments [5]–[7]. The purpose of the present paper is to report the observation of a large number of magnetostatic mode resonances in axially magnetized cylindrical rods of polycrystalline yttrium iron garnet at 9.96 GHz which can be satisfactorily explained on the basis of magnetostatic mode theory for rods in air [6] and rods encased in metal sleeves [8]. In Section II the details of the experiment are summarized and the experimental results described. In Section III the details of magnetostatic mode theory which are relevant to the theoretical interpretation of the data are presented. The data are then compared with the theoretical predictions in Section IV, and the results of the investigation are summarized in Section V.

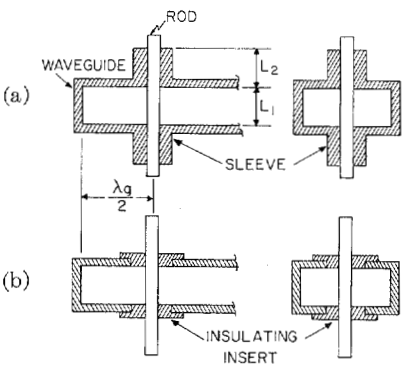

Fig. 2. Shorted waveguide sections and sample support arrangements which were used to obtain absorption curves. (a) Rod supported by metal sleeves of length L_2 outside waveguide. (b) Rod supported by insulating inserts.

II. Experiment

Magnetostatic mode resonances were observed using a microwave spectrometer at 9.96 GHz, as shown in Fig. 1. A stabilized klystron was used to provide microwave excitation to the axially magnetized rod placed one-half wavelength from a TE_{10} waveguide short. The power reflected from the short was detected, and a voltage proportional to this power was displayed on the y axis of a pen recorder. A Hall effect magnetic field probe was used to monitor the static magnetic field along the rod axis and drive the x axis of the recorder. The rods were machined to 0.075-inch diameter, from polycrystalline yttrium iron garnet with a linewidth of 25 Oe at 9.96 GHz, as measured on spherical samples. The 75-mil diameter rods were inserted through holes in the waveguide centered in the wide faces of the waveguide walls, thereby providing a uniform microwave field over that portion of the rod inside the waveguide perpendicular to the rod axis and the static magnetic field.

The nature of the absorption curve (difference between incident power and reflected power as a function of static field) was found to depend strongly on the manner in which the rod was supported at the waveguide walls. In Fig. 2 the two support techniques which were used are shown schematically by means of waveguide cross-sectional views. The first arrangement [Fig. 2(a)] provided rod support by means of two snug-fitting metal sleeves 1 inch in length on each side of the waveguide. The second [Fig. 2(b)] provided rod support by means of insulating spacer inserts so that no metal surface was in close proximity to the rod. A third configuration, not shown in Fig. 2, consisted of two snug-fitting holes in the waveguide wall.

Absorption spectra were obtained using the technique and rod support arrangements described above. These results for a YIG rod 3 inches long are shown in Fig. 3. The spectra indicated by the solid curve in Fig. 3 correspond to the sleeve supported rod configuration of Fig. 2. The spectra consist of a series of about 15 weak resonances extending from 1800 to 2600 Oe, a main peak at about 2725 Oe, and a series of resonances beyond the main peak extending out to 3400 Oe. In the spectra for the insert-supported rod, the weak resonances from 1800 to 2600 Oe disappear as indicated by the dotted line in the figure, but the other resonances are identical with those for the sleeve-supported rod. The differences in absorption curves for the two cases indicate that 1) the resonances between 1800 and 2600 Oe are associated with those portions of the rod that are enclosed in the metal sleeves, and 2) the main peak at 2725

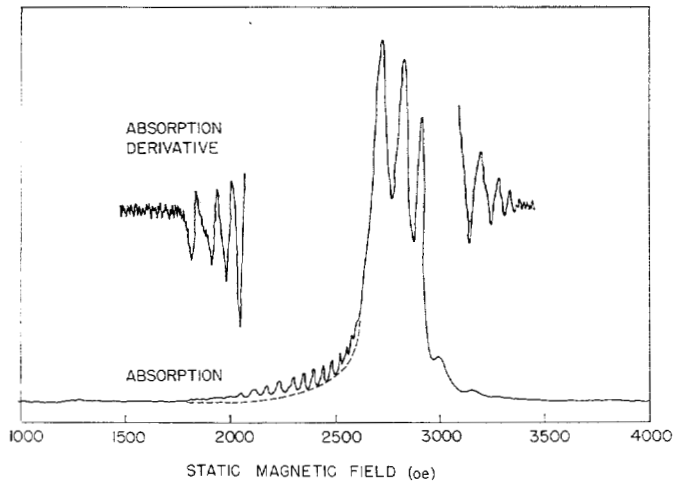

Fig. 3. Absorbed energy as a function of static magnetic field at 9.96 GHz for a 0.075-mil diameter 3-inch long YIG rod obtained using the two support arrangements of Fig. 2. The solid curve corresponds to the metal sleeve supports, the dotted line indicates modifications of spectra obtained for an insert-supported rod.

Oe and those at higher fields are associated with that portion of the rod which is inside the waveguide structure.

Several other experiments were performed to check these two conclusions. An absorption curve was obtained with the rod supported by snug-fitting holes in the waveguide wall. The curve was identical to that for the insert-supported rod, except for a strong resonance at about 2400 Oe. The resonances at 2725 Oe and above were unchanged. The spectra for the sleeve-supported arrangement were obtained for rods of different length. As long as the rod was sufficiently long to extend completely through both sleeves, the spectra were identical with the solid curve in Fig. 3. For rods too short to fill both sleeves but long enough to extend through the waveguide, the positions of the weak resonances below the main peak were shifted to higher fields still below the main peak, but the main peak and resonances at higher fields were identical to those in Fig. 3. If the rod were placed as to extend only part way into the waveguide, the resonances at 2725 Oe and above would be modified severely. The various spectra obtained by changing the rod length, position, and support technique confirm the above association of the weak resonances from 1800 to 2600 Oe with the sleeve-supported portions of the rod and those at 2725 Oe and above with the portion of rod in the waveguide. In addition to these qualitative associations, it has been found that the absorption spectra of Fig. 3 can be quantitatively explained on the basis of magnetostatic mode theory, in a manner entirely consistent with these conclusions. After a brief review of magnetostatic mode theory, a quantitative comparison will be made.

III. Theory

The magnetostatic mode spectra for long axially magnetized rods in air has been calculated by Joseph and Schlömann [6] by simultaneously solving Maxwell's equations and the magnetic torque equation, neglecting electromagnetic propagation effects, exchange forces, and magnetic losses. Such a calculation is valid as long as the wavelengths of the resultant modes are smaller than the electromagnetic wavelength at the same frequency in the medium and large enough so that the exchange contribution to the mode energy is negligible. In this section, several aspects of the Joseph and Schlömann theory which are relevant to the present data will be reviewed; the discussion will be extended to include magnetostatic modes for cylindrical rods encased in metal sleeves (treated briefly in [8]), and the factors that determine which of the allowed modes are most likely to be excited in the present experiment will be considered.

Following [6], the microwave magnetic field $\boldsymbol{h}$ in the rod can be represented as the gradient of a magnetostatic potential Ψ which is of the form

$$\Psi = \psi(\rho)e^{-i(\beta z+m\phi)} \tag{1}$$

in cylindrical coordinates (ρ, ϕ, z) with z along the rod axis. Here m is an integer, and the propagation constant β can have an arbitrary value. Inside the rod $\psi(\rho)$ is of the form

$$\psi(\rho) = J_m[|\beta|\rho(-\mu)^{1/2}] \tag{2}$$

where J_m is an mth order Bessel function of the first kind and μ is the diagonal element of the permeability tensor given by

$$\mu = [H(H + 4\pi M) - (\omega/\gamma)^2]/[H^2 - (\omega/\gamma)^2]. \tag{3}$$

Here H is the static field in the axial direction, $4\pi M$ is the saturation induction, ω is the angular excitation frequency, and γ is the gyromagnetic ratio. Outside the rod, $\psi(\rho)$ is of the form

$$\psi(\rho) = cK_m(|\beta|\rho) \tag{4}$$

where K_m is a modified Bessel function of the second kind and c is determined by the continuity condition on the tangential component of $\boldsymbol{h}$ at the rod surface. The remaining boundary condition, the continuity of the normal component of $\boldsymbol{h} + 4\pi\boldsymbol{m}$, where $\boldsymbol{m}$ is the microwave component of the magnetization, leads to a characteristic equation which determines the allowed magnetostatic mode frequencies (for a given field) or mode field positions (for fixed frequency) as a function of m (an integer) and reduced wave number $|\beta|R$ where R is the rod radius. The details of the characteristic equation derivation and solutions are given in [6]. Two types of solutions are obtained, so-called volume modes and surface modes.

Volume modes are confined to the field region

$$\sqrt{(2\pi M)^2 + (\omega/\gamma)^2} - 2\pi M < H < \omega/\gamma \tag{5}$$

for which μ is negative and the argument of J_m in (2) is real. For a given value of frequency (or field) m and reduced wave number $\zeta = |\beta|R$, an infinite number of solutions are possible, corresponding to the zeros $j_{m1}, j_{m2}, \cdots, j_{mr}, \cdots$, of J_m. Solutions exist for both positive and negative m. In the limits $\zeta \to 0$ and $\zeta \to \infty$, all solutions converge to the lower and upper limits of (2), respectively. Neither of these limits is strictly allowed, however, because of the previ-

ously mentioned neglect of electromagnetic propagation effects and exchange forces.

For rods in air, surface modes are confined to the field region

$$(\omega/\gamma) - 2\pi M < H < \sqrt{(2\pi M)^2 + (\omega/\gamma)^2} - 2\pi M \quad (6)$$

for which μ is positive and the argument of J_m in (2) is imaginary. At large distances from the center of the rod, therefore, the potential Ψ increases exponentially, and the excitation is primarily confined to the surface of the sample; hence the name *surface mode*. The significance of the surface modes was first pointed out by Eshbach and Damon [9]. The Joseph and Schlömann calculation shows that surface modes for rods in air are allowed only for positive m and a reduced wave number less than a cutoff value ζ_m defined by

$$K_m'(\zeta_m)/K_m(\zeta_m) + (m/\zeta_m)[(H + 4\pi M)/H]^{1/2} = 0 \quad (7)$$

where the prime denotes differentiation with respect to the argument of K_m. For given values of m and ζ, one surface mode solution is possible if the condition $\zeta < \zeta_m$ can be satisfied within the field limits of (6). Otherwise, no solutions are allowed. Note that ζ_m is independent of frequency and determined only by the angular mode index m and the ratio $(H + 4\pi M)/H$.

In the Joseph and Schlömann calculation, the characteristic equation was solved in such a way as to obtain the frequency values at which the allowed volume or surface modes resonate for a given value of static magnetic field. In most experiments the frequency is fixed and the field is the adjustable parameter, so that it is more desirable to obtain the values of field at which the allowed modes resonate for a given value of frequency. For volume modes, the characteristic equation of Joseph and Schlömann can be written as

$$\frac{J_{m-1} - J_{m+1}}{J_{m-1} + J_{m+1}} + s^2 \frac{K_{m-1} + K_{m+1}}{K_{m-1} - K_{m+1}} = -\frac{s^2}{\sigma}\left[\sqrt{1 + \sigma^2\left(\frac{1 + s^2}{s^2}\right)^2} + 1\right] \quad (8)$$

where

$$\sigma = \omega/\gamma^2\pi M$$

$$J_m = J_m(\zeta s)$$

$$K_m = K_m(\zeta).$$

For given values of ζ, $4\pi M$, and ω, (8) can be solved for s. An infinity of solutions exists. The volume mode solution corresponding to the rth zero of J_m is obtained with the additional restriction that

$$j_{|m|,r-1} < s\zeta < j_{|m|,r}$$

if m is positive, or

$$j_{|m|,r} < s\zeta < j_{|m|,r+1}$$

if m is negative. The value of applied field at which the volume mode (σ, ζ, m, r) resonates can be obtained from

$$\gamma H/\omega = \frac{1}{\sigma}\frac{s^2}{1 + s^2}\left[\sqrt{1 + \sigma^2\left(\frac{1 + s^2}{s^2}\right)^2} - 1\right]. \quad (9)$$

The solution for surface modes is obtained by noting that $J_m(i\zeta|s|) = i^m I_m(\zeta|s|)$, where the I_m are modified Bessel functions of the first kind, and that $s^2 < 0$ is satisfied for surface waves. Thus the relevant characteristic equation is obtained from (8) by replacing $J_{m+1}(\zeta s)$ by $I_{m+1}(\zeta|s|)$ and $J_{m-1}(\zeta s)$ by $-I_{m-1}(\zeta|s|)$. The characteristic equation is then solved for $s^2 < 0$, and the field strength at which the mode resonates is calculated from (9). As mentioned previously, surface mode solutions are allowed only for $m > 0$ and $\zeta < \zeta_m$.

The preceding discussion has been concerned with the mode spectra for rods in air. For rods enclosed in metal sleeves, it is reasonable to impose the boundary conditions which are applicable in the case of perfectly conducting sleeves, i.e., the normal component of $\boldsymbol{h} + 4\pi\boldsymbol{m}$ must vanish at the rod surface. No boundary condition is imposed on the tangential component of $\boldsymbol{h}$ because the microwave magnetic field is shielded by surface currents in the perfect conductor surrounding the sample. The characteristic equation for rods in metal sleeves is the same as for rods in air, except that the term involving K_{m+1} and K_{m-1} in (8) is deleted. As for rods in air, surface waves are allowed only for positive m. There is no cutoff wave number, and the lower limit of the allowed field range in (6) is lowered by $2\pi M$. The analysis in Section IV shows that it is the surface modes that are relevant to the data, and volume modes for rods in metal sleeves will not be considered here.

In the preceding treatment the wave number β is arbitrary because the rod is assumed to be infinitely long. In the experiment, however, resonances are observed which are supported by finite portions of the rod of length L_1 or L_2, as discussed in the Section II. The wave numbers corresponding to these resonances form a discrete sequence. Their precise magnitude depends upon the boundary conditions at the ends of the mode-supporting part of the rod. A rigorous formulation of these boundary conditions is quite difficult and outside the scope of the present paper. As a first approximation, the allowed values of β can be assumed to be integer multiples of $\pi/L_{1,2}$. This assumption implies that the allowed modes are standing wave resonances with an integral number of half wavelengths along the mode-supporting portions of the rod.

The nature of the various allowed magnetostatic mode resonances in axially magnetized rods has been described, and a formula has been given for calculating the mode field positions as a function of frequency, wave number, angular index m, and radial index r (r applies to volume modes only). In addition, it is important to consider which of the many allowed modes are likely to be strongly excited under the excitation conditions which exist in the present experiment, namely, a uniform microwave field normal to

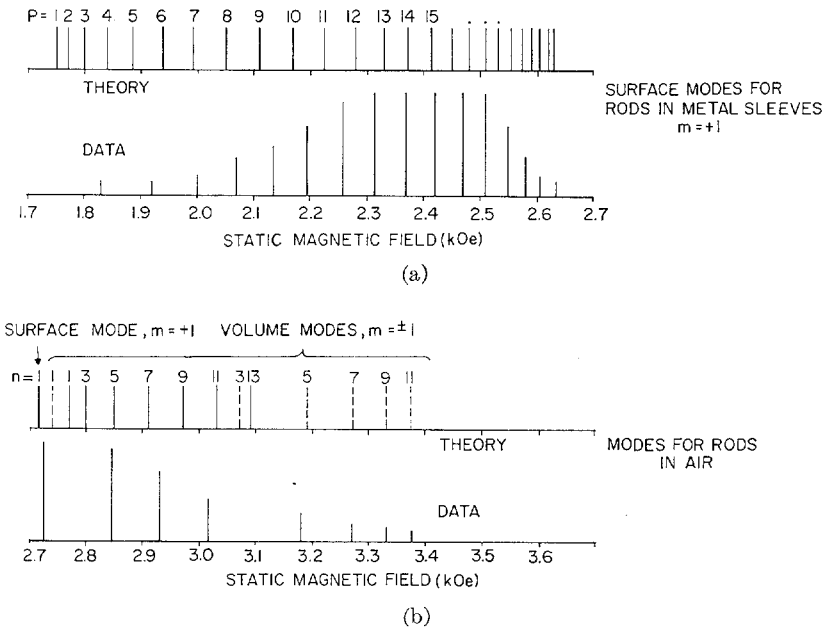

Fig. 4. Schematic representation of the field positions of the absorption peaks and theoretical resonance positions calculated as explained in text. (a) Series of weak resonances below main peak in Fig. 3. (b) Main peak at 2725 Oe and the series of resonances at higher field.

the rod axis which extends over the length of the rod in the waveguide. Such considerations are necessary in order to decide which mode positions should be calculated for comparison with the experimental data. The following discussion is intended to provide a few qualitative criteria for strong mode excitations. A detailed treatment of mode coupling to external microwave fields is beyond the scope of this paper.

One qualitative criterion for strong coupling is a good match between the external microwave field and the mode field over the mode-supporting portion of the rod. The external microwave field is uniform over the rod cross section. From $h_\rho = \partial\Psi/\partial\rho$, $h_\phi = (1/\rho)(\partial\Psi/2\phi)$, and (1) and (2), the mode field $\boldsymbol{h}$ is most nearly uniform over the rod cross section for $|m| = 1$, small values of $|\beta|R|\mu|^{-1/2}$, and small r (for volume modes). For modes supported in the portion of the rod in the waveguide, of length L_1, the external microwave field is uniform over the length L_1. Only modes with an odd integral number of half wavelengths along L_1 can be excited. These modes satisfy the requirement $|\beta| = n\pi/L_1$ $(n = 1,3,5\cdots)$. The strongest coupling is expected for the low-order $n = 1$ mode. For the modes supported in the sleeve enclosed portions of the rod, of length L_2, the external microwave field is large only at the waveguide end of the sleeve. Modes with $|\beta| = p\pi/L_2$ $(p = 1,2,3,\cdots)$, where p is any integer, can be excited. However, the external microwave field penetrates the sleeve-enclosed portions of the rod a distance on the order of the rod diameter. Therefore, the strongest coupling is expected for modes with $|\beta|$ on the order of the inverse rod diameter.

These qualitative criteria will be used as a basis for calculating expected mode positions for comparison with the data in Section IV. They will also be used as a basis for estimating which resonances should be strong and which should be weak.

IV. Results and Discussion

The field positions of the resonance peaks shown in Fig. 3 were measured to ±1 Oe using a Hall effect gaussmeter calibrated with a nuclear magnetic resonance spectrometer. The experimental mode positions were compared with theoretical positions calculated using the formula described in Section III. Surface mode positions for rods in metal sleeves were evaluated for $m = +1$ and $|\beta| = p\pi/L_2$ $(p = 1,2,3,\cdots)$. Surface mode positions were also calculated for rods in air with $m = +1$ and $|\beta| = n\pi/L_1$ $(n = 1,3,5,\cdots)$ but below cutoff. Volume mode positions were calculated for rods in air with $m = \pm 1$, $r = 1,2,3,\cdots$, and $|\beta| = n\pi/L_1$. The following parameters were used: $R = 0.0375$ inch, $L_1 = 0.4$ inch, $L_2 = 10$ inch, $\omega/2\pi = 9.96$ GHz, $\gamma = 1.76 \times 10^7$ Oe$^{-1}\cdot$s^{-1}, and $4\pi M = 1809$ gauss. The saturation induction $4\pi M$ was determined with a vibrating sample magnetometer on a 1-mm diameter sphere obtained from the rod material.

In Fig. 4 the experimental peak positions are compared with the theoretical values. The resonances are indicated schematically by vertical lines at the appropriate field values. The intensities for the experimental peaks are qualitatively indicated by the length of the lines representing individual resonances. Spectra diagrams shown in Fig. 4(a) are for the series of resonances below the main peak, and the theoretical positions correspond to surface modes for rods enclosed in metal sleeves with $m = +1$. The values of p used to label the modes correspond to the number of half wavelengths across the sleeve length L_2.

Diagrams shown in Fig. 4(b) are for the main peak and the series of resonances above the main peak. The theoretical mode positions correspond to surface modes for rods in air with $|\beta| = m\pi/L_1$, as shown by the heavy line (only the $n = 1$ mode was below cutoff), volume modes for rods in air with $m = -1$ (solid lines), and volume modes for rods in air with $m = +1$ (dotted lines).

First consider the results shown in Fig. 4(a) for the resonances associated with the sleeve-enclosed rod sections. The mode spacings are in fairly good agreement with the theory, except for the low-order modes ($p = 1$–4) and extremely high-order modes ($p > 17$). The experimental peaks appear to be shifted to slightly higher fields than expected theoretically. The comparison indicates that the strongest resonances correspond to modes with 12–16 half wavelengths over the sleeve length. For these modes, a half wavelength is on the order of the penetration depth of the microwave field into the sleeve, a distance on the order of $2R$, so that the intensity peak is consistent with the qualitative criteria for strong mode excitation discussed in Section III. Modes with wavelengths on the order of the excitation length are expected to be strongly excited. The shift of the experimental peaks with respect to the theoretical positions can be seen more clearly by displaying the mode separation as a function of static magnetic field, as shown in Fig. 5. For modes with $8 < p < 18$, the shape of the theoretical curve is closely matched by the data, except that the experimental curve is shifted to higher field by about 100 Oe. It is important to realize that the theory is strictly valid only if the rod is surrounded by a perfect conductor that is everywhere in contact with the sample. A perfectly tight fit of the rod in the sleeve is not possible experimentally, and it is reasonable to assume the existence of a small airspace between the rod and sleeve. Insofar as air boundary conditions shift the lower field limit for surface modes upward by $2\pi M$, with a corresponding upward shift in the mode positions, it is suggested that the 100-Oe shift is largely due to a small airspace between the rod and sleeve. The fact that the sleeves are actually metal and not perfect conductors, as assumed in the theory, may also be partially responsible for the shift of the modes to higher fields. Finally, it is also conceivable that a more rigorous consideration of the boundary conditions at the ends of the metal sleeve will modify the allowed values of β sufficiently to influence the theoretical mode positions in Fig. 4(a). The theoretical spectrum has also been evaluated for $|\beta| = p\pi/(L_2 \pm R)$. The results indicate that a decrease in the length of the mode-supporting region can also partially explain the field shift evident in Fig. 5. The increased mode spacings for the low-order modes with $p < 8$ are not presently understood. Because of their long wavelength, the magnetostatic approximation may not be valid for these modes.

Next consider the results for the resonances associated with the portion of the rod inside the waveguide, as shown in Fig. 4(b). For YIG at 9.96 GHz, the only $m = +1$ surface mode which is not beyond cutoff is that for which $|\beta| = \pi/L_1$, corresponding to one-half wavelength over the portion of the rod inside the waveguide. The theoretical mode position of 2715 Oe shown by the heavy line in Fig. 4(b) compares quite favorably with the position of the main peak at 2725 Oe. The uniform precession mode in a rod whose cross section is very small compared to its length is essentially a surface mode [6]. For $|\beta| = 0$, this resonance is expected at 2650 Oe. The peak at 2725 Oe corresponds to this uniform precession resonance expected for long cylinders which are removed from all metal boundaries. In the present case this mode is not entirely uniform, but has an axial wavelength of twice the waveguide height, which accounts for the observed 75-Oe shift of the resonance to higher field. The series of resonances on the high-field side of the main peak are also associated with the portion of rod inside the waveguide. For this series of resonances, theoretical mode positions are shown for $m = \pm 1$ (dotted and solid lines, respectively) and $r = 1$. The resonance peaks between 3100 and 3400 Oe, shown in Fig. 4(b), agree quite well with the theoretical mode positions for volume modes with $m = 5, 7, 9, 11$. The theoretical mode spacing decreases with increasing r so that low-order resonances for larger r should merely contribute to the background absorption. In fact, this is the primary effect of the modes for $r > 1$ and accounts for the high level of background absorption between 2700 and 3000 Oe. The three low-field lines between 2800 and 3000 Oe do not appear to correspond to any of the theoretical modes. The predicted higher-order modes in this field region are expected to be only weakly excited and are probably obscured by the background absorption. It is possible that the low-order modes, like the low-order surface modes for rods in sleeves, are more widely separated than expected from theory. Electromagnetic propagation effects [10], which are neglected in the magnetostatic theory, may be important for these low-order long wavelength modes.

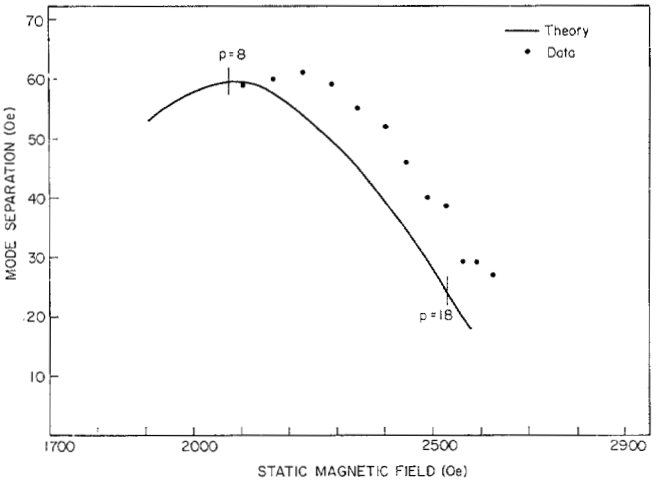

Fig. 5. Mode separation as a function of static magnetic field. Solid curve was calculated for surface modes in rods with metal boundary conditions at the rod surface. Solid points correspond to the series of resonances below the main peak in Fig. 3.

V. Conclusion

The magnetostatic mode spectra for axially magnetized polycrystalline rods at 9.96 GHz has been observed experimentally. Two distinct series of modes were observed. The first series of modes occurred at fields between 1800 and 2600 Oe and is associated with portions of the rod that are outside the waveguide structure and supported by metal sleeves. It has been found that these resonance positions can be explained on the basis of magnetostatic mode theory for surface modes in rods with metal boundary conditions. The second series of modes between 2700 and 3500 Oe is associated with the portion of the rod inside the waveguide structure. The strongest resonance was observed to occur at 2725 Oe. It corresponds to the uniform precession resonance expected at 2650 Oe for long rods far removed from metal boundaries. The resonance is shifted to higher field because the mode is actually a surface magnetostatic mode with a wavelength equal to twice the waveguide height. The resonances on the high-field side of the main peak can be identified with volume modes in the portions of the rod inside the waveguide.

The primary results of this investigation are 1) the observation of a large number of magnetostatic mode resonances in axially magnetized YIG rods using a short-circuited waveguide technique; 2) the correlation of the observed spectra with magnetostatic mode theory of surface modes for rods in air or in metal sleeves, and volume modes for rods in air.

Acknowledgment

The authors wish to thank E. Q. Maguire for providing the samples for the experimental investigation and Miss W. Doherty for assistance in the numerical calculations.

References

[1] A. W. Trivelpiece, A. Ignatius, and P. C. Holscher, "Backward waves in longitudinally magnetized ferrite rods," *J. Appl. Phys.*, vol. 32, pp. 259–267, February 1961.
[2] F. A. Olson and J. R. Yaeger, "Microwave delay techniques using YIG," *IEEE Trans. Microwave Theory and Techniques*, vol. MTT-13, pp. 63–69, January 1965.
[3] F. A. Olson, E. K. Kirchner, K. B. Mehta, F. J. Peternell, and B. C. Morley, "Propagation of magnetostatic surface waves in YIG rods," *J. Appl. Phys.*, vol. 38, pp. 1218–1220, March 1967.
[4] M. Bini, L. Millanta, N. Rubino, and I. Kaufman, "Magnetostatic waves in axially magnetized cylinders: experimental dispersion curves," *Nuovo Cimento*, vol. 47, pp. 281–293, February 1967.
[5] P. C. Fletcher and C. Kittel, "Considerations on the propagation and generation of magnetostatic waves and spin-waves," *Phys. Rev.*, vol. 120, pp. 2004–2006, December 1960.
[6] R. I. Joseph and E. Schlömann, "Theory of magnetostatic modes in long, axially magnetized cylinders," *J. Appl. Phys.*, vol. 32, pp. 1001–1005, June 1961.
[7] B. A. Auld and K. B. Mehta, "Magnetostatic waves in a transversely magnetized rectangular rod," *J. Appl. Phys.*, vol. 38, pp. 4081–4083, September 1967.
[8] K. Mehta and F. A. Olson, "Investigations of broadband ferromagnetic power limiters and expanders as duplexing elements for microwave systems," U. S. Army Electronics Command, Fort Monmouth, N. J., Contract DA-28-043-AMC-02120(E), 1st Quart. Prog. Rept., December 1966.
[9] J. R. Eshbach and R. W. Damon, "Surface magnetostatic modes and surface spin waves," *Phys. Rev.*, vol. 118, pp. 1208–1210, June 1960.
[10] B. A. Auld, "Coupling of electromagnetic and magnetostatic modes in ferrite-loaded cavity resonators," *J. Appl. Phys.*, vol. 34, pp. 1629–1633, June 1963.